Optical and x-ray diffraction studies on the incorporation of carbon as a dopant in cubic GaN

J. R. L. Fernandez, F. Cerdeira, E. A. Meneses, and M. J. S. P. Brasil
Instituto de Física "Gleb Wataghin," Universidade Estadual de Campinas, Caixa Postal 6165, 13083-970 Campinas, São Paulo, Brazil

J. A. N. T. Soares,* A. M. Santos, O. C. Noriega, and J. R. Leite
Instituto de Física, Universidade de São Paulo, Caixa Postal 66318, São Paulo, São Paulo, Brazil

D. J. As, U. Köhler, S. Potthast, and D. G. Pacheco-Salazar
Universität Paderborn, FB-6 Physik, D-33095 Paderborn, Germany
(Received 28 February 2003; revised manuscript received 26 June 2003; published 17 October 2003)

We performed optical and x-ray diffraction experiments on carbon doped cubic-GaN samples, deposited by plasma-assisted molecular beam epitaxy on (001) GaAs substrates, for various carbon concentrations. The samples were studied by Raman, photoluminescence, and photoluminescence excitation spectroscopies. These techniques give some insight into the mechanism of carbon incorporation in the material. Detailed analysis of these spectra leads to a picture in which carbon initially enters into N vacancies producing a marked improvement in the crystalline properties of the material. At higher concentrations it also begins to enter interstitially and form C complexes, with a consequent decrease of crystalline quality. This increase and later decrease of crystalline quality of our samples with the addition of C were also detectable in x-ray diffraction scans. A model calculation of the localized vibrations of the C atom in the GaN lattice allows for the interpretation of a feature in the Raman spectrum of some samples, which reinforces this view.

DOI: 10.1103/PhysRevB.68.155204 PACS number(s): 78.20.−e, 78.30.Fs, 78.55.Cr

I. INTRODUCTION

The metastable cubic modification of GaN has attracted a lot of attention for its potential optoelectronic applications, especially since the successful fabrication of light-emitting diodes based on structures constructed with this material.[1–6] In contrast to the stable wurtzite variety, no spontaneous polarization or strain-induced piezoelectric field exists in the cubic polytype grown on (001) planes. Hence, there is no piezoelectric-field-induced spatial separation between electron and hole wave functions, which should lead to a greater optical recombination efficiency in quantum wells based on cubic GaN. For the fabrication of devices with this material, it is essential to be able to introduce *p*- and *n*-type dopings in a controlled manner. This involves introducing dopant impurities, which produce shallow acceptor or donor levels. Understanding how these impurities enter into the GaN lattice is of fundamental importance for achieving useful doping. Among the possible acceptor impurities, carbon has been regarded as an interesting candidate due to its similarity with nitrogen, both in atomic radius and electronegativity. Limited success in using this dopant was reported earlier on by Abernathy *et al.*[7] However these authors used CCl_4, which limited the hole concentration to a maximum of 3×10^{17} cm^{-3}. More recently As reported *p*-type doping with carbon by *e*-beam evaporation of a carbon rod during the molecular beam epitaxy (MBE) growth of cubic-GaN.[8,9] Here carbon concentrations reached levels of the order of 3×10^{20} cm^{-3}. In order to understand how this concentration translates itself into a high concentration of mobile holes, the details of the incorporation of C in the GaN lattice must be understood.

In the present paper we report optical and x-ray diffraction studies of cubic-GaN samples, deposited by plasma-assisted MBE on (001) GaAs substrates, doped with different carbon concentrations. The samples were studied by Raman, photoluminescence (PL), and photoluminescence excitation (PLE) spectroscopies. The evolution of these spectra is consistent with a picture in which carbon enters into N vacancies at low concentrations, thus producing a marked improvement in the crystalline properties of the material. At higher concentrations it also begins to incorporate at non-substitutional sites and form carbon complexes, with a consequent decrease of crystalline quality. This view is reinforced by the observation of a line (at 584 cm^{-1}) in the Raman spectra of the samples with relatively large amounts of carbon and best crystalline quality. Based on a valence force field calculation, we attribute this line to a resonance vibration of C atoms occupying N sites in the cubic GaN lattice.

II. EXPERIMENT

Cubic GaN films were grown by rf-plasma assisted MBE on semi-insulating (001) GaAs substrates at a temperature of 720 °C.[10,11] The growth rate was of 0.07 μm/h and the total thickness of each film was ≈ 1 μm. Carbon doping was achieved, as explained in detail in Ref. 8, by electron-beam evaporation of a graphite rod, with the *e*-beam power maintained constant between 0 and 400 W during the growth. The C flux was calibrated by growing C-doped GaAs in the same manner and assuming the same sticking coefficient for C on GaAs and GaN. Secondary ion mass spectroscopy was used in some samples to confirm this calibration (see Ref. 8). This procedure shows that C content increases monotonically with *e*-beam power. The samples used in our experiment are labeled *A* through *G* in order of increasing carbon content and listed with their estimated C concentration in Table I. All samples were found to be *p*-type by Hall measurements.[8]

TABLE I. List of samples used in our experiments with their thickness and ordered according to their carbon content. The amount of carbon incorporated ([C]) is estimated from the evaporating *e*-beam power used during growth.

Sample	Thickness (nm)	*e*-beam power (W)	[C] (cm^{-3})	$E_{exc}(\Gamma_{exc})$ (eV) (meV)	$E_g(\Gamma_g)$ (eV) (meV)	$2\theta(\Gamma)$ (deg)
*A*1	185	0	Undoped		3.26 (50)	39.758 (0.961)
*A*2	659	0	Undoped	3.299 (56.5)	3.325 (39.5)	39.924 (0.338)
*A*3	631	0	Undoped	3.294 (60.3)	3.325 (36.0)	39.921 (0.383)
B	1030	70	2×10^{17}	3.288 (49.2)	3.314 (21.2)	
C	1035	90	2.5×10^{17}			39.921 (0.276)
D	1121	150	4×10^{17}	3.295 (54.9)	3.321 (33.1)	39.922 (0.219)
E	728	200	8×10^{17}	3.292 (60.0)	3.318 (43.7)	39.922 (0.280)
F	676	280	3×10^{18}	3.285 (60.8)	3.311 (57.8)	(0.323)
G	677	350	1.5×10^{19}	3.285 (65)	3.311 (52.9)	39.921 (0.319)

The crystalline quality of the samples was evaluated by high-resolution x-ray diffraction (HR-XRD). The measurements were carried out using the Cu $K\alpha$ radiation ($\lambda = 1.540\,597$ Å) in a Philips X'pert four-circle Materials Research Diffractometer in triple axis configuration yielding a resolution better than 20 arcsec. We measured ω-2θ scans of the symmetric (002) reflection of the layers (ω is the angle of incidence and θ is the Bragg diffraction angle).

Both PL and PLE spectra were excited with an air-cooled 1000-W Xe lamp filtered with a 1.0-m SPEX monochromator with a 1200 groove/mm grating. The monochromatic light was focused onto the sample, contained in an Air Products cold finger cryostat at $T=10$ K. Emitted light was focused onto a double monochromator with a Ga-In-As photomultiplier tube. Quartz lenses were used both for excitation and for collection of emitted radiation. The excitation wavelength used for the PL experiments was 329 nm.

Unpolarized micro-Raman measurements were made (at $T=10$ K) in the backscattering configuration, using $\sim 1.5\times10^4$ W/cm^2 of the 514.5-nm line of an argon-ion laser as exciting radiation. Scattered light was analyzed with a triple Jobin-Yvon T-4000 *XY* spectrometer equipped with a multichannel charge-coupled device. An optical microscope with a $\times 50$ objective was used to focus the laser beam on the sample and collect the scattered light. The laser spot on the sample was between 1 and 2 μm in diameter. The spectral resolution was between 1 and 2 cm^{-1}.

III. RESULTS AND DISCUSSION

Figure 1 displays the Raman spectra of some of the intentionally doped samples. The spectra are characterized by sharp two peaks originating in the TO (555 cm^{-1}) and LO (741 cm^{-1}) phonons of *c*-GaN (Ref. 12) and a broad continuum between these lines. A discrete line at 568 cm^{-1} (designated as E_2 in this figure) appears in some spectra and is due to one-phonon scattering by inclusions of the hexagonal phase of the material. The broad continuum is also observed in the Raman spectra of related compounds, such as AlGaN alloys, and is attributed to scattering by phonon density of states activated by disorder (defects, dislocations, and other crystalline imperfections), which destroys the *k*-conservation rule.[13] The spectra in Fig. 1 clearly show a marked decrease in the relative intensity of this broad continuum as more carbon is incorporated in the sample (higher *e*-beam power). This indicates that disorder decreases with increasing carbon concentration. This can only be explained as an increase in crystalline quality, since the presence of an extraneous atom (C) in the GaN network would, in principle, increase disorder and not the other way around. To understand this effect, let us first notice that all of our samples were grown on Ga-rich conditions in order to stabilize the cubic metastable phase.[10] Under this condition the very high nitrogen equilibrium pressure at growth temperatures favors the appearance of nitrogen vacancies. Our undoped samples (*A*1, *A*2, and *A*3) display a hole concentration *p* of about 10^{16} cm^{-3} and, therefore, have the Fermi level at the lower half of the GaN band gap. This, in turn, strongly favors the formation of N vacancies, as shown in Refs. 14 and 15, making them the dominant type of defect on these samples. These vacancies produce lattice distortions around them, which could be largely responsible for the break in periodicity originating the broad continuum in the Raman spectrum. If the carbon atoms occupy the sites of these vacancies, the

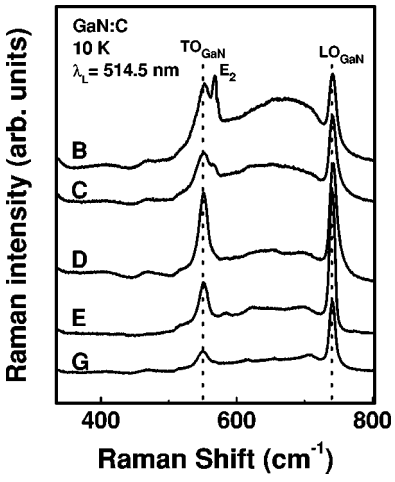

FIG. 1. Raman spectra of C-doped cubic GaN for different *e*-beam powers used during growth. Higher power corresponds to a higher C concentration.

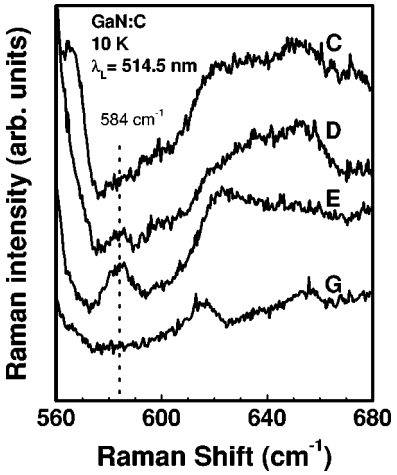

FIG. 2. Raman spectra of C-doped cubic GaN for different C concentrations, showing the structure at 584 cm^{-1} present in the spectra of samples *D* and *E*.

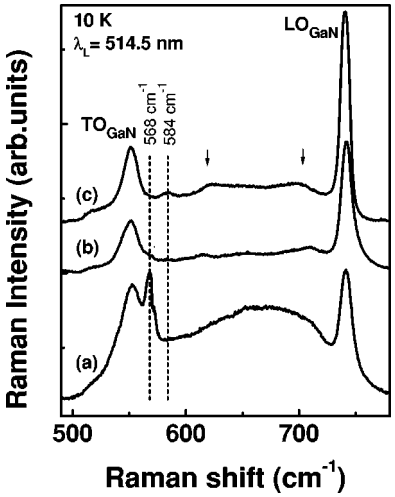

FIG. 3. Raman spectra from three cubic GaN samples: C doped grown with an *e*-beam power of 70 W (a) (sample *B*); As-doped (b) (not in Table I); and C doped grown with an *e*-beam power of 200 W (c) (sample *E*). The vertical dotted lines mark the peaks arising from hexagonal inclusions in (a) and from the resonance vibration of a C atom in the GaN lattice in (c). The arrows point to structures arising from defects common to C- and As-doped samples.

crystalline distortions disappear due to the similarities in the atomic radii of N and C. Therefore, at concentrations where the random substitution of N by C atoms does not constitute a serious source of disorder (less than 1% or so) the inclusion of C results in an improvement of the crystalline quality of the material which, in turn, causes the defect-related structure in the Raman spectrum to be quenched. Thus, the evidence in Fig. 1 gives a strong indication about the sites occupied by the C dopants.

The Raman spectrum of the material would give additional insights in to the carbon incorporation in GaN if a given spectral feature could be attributed to a localized vibration of the carbon atom. An impurity with a much smaller mass than either of the host atoms would give rise to a truly localized vibration, i.e., one with a frequency in the forbidden region of the host lattice vibrations and whose amplitude is large at the impurity-site and decreases rapidly with increasing distance to it. If, as in this case, the impurity atom has a mass similar to one of the host atoms, the vibrational mode introduced by the impurity is a resonance mode, with a frequency contained in the range of the allowed modes of the perfect crystal and an amplitude that falls off slowly as we move away from the site of the impurity atom.[16] These modes are difficult to observe, unless their frequency happens to lie at a point where the density of states of the vibrations of the pure crystal is small. To the best of our knowledge, all previous attempts to find direct evidence of such C-related modes in the Raman spectrum of GaN:C have yielded no positive results.[17,18] However, we believe that the Raman spectra of some of our GaN:C samples show evidence of the existence of this type of mode. In Fig. 1 a structure at 584 cm^{-1} appears in the spectra from the two samples (*D* and *E*) with the best crystalline quality, which are reproduced in Fig. 2 in a more convenient scale. Here we observe that the weak line at 584 cm^{-1} starts to be visible for sample *D*, and gains strength as C concentration increases up to the point where the C complexes begin to form. In the most doped samples, where the C complex related emission at 2.1 eV dominates the PL spectra (see Fig. 5, sample *G*), this line is completely quenched.

Finally, in Fig. 3 we show the Raman spectra of two carbon-doped samples grown with an *e*-beam power of 70 W (a) and 200 W (c) and that of an As-doped one (b), in the spectral region between the TO and LO modes of the GaN. In this region, the spectrum of the C-doped sample grown with a low *e*-beam power (a) exhibits a peak at 568 cm^{-1} due to hexagonal inclusions and a very broad continuum which results, as previously discussed, from the poorer crystalline quality of these samples. This broad continuum is replaced by a more structured one in both, the As-doped sample (b) and the C-doped sample (c). When comparing these curves, we notice a series of common features (between 620 and 700 cm^{-1}) as well as a peak at 584 cm^{-1}, which appears only in the carbon-doped sample. This cannot be attributed to hexagonal inclusions seen in curve (a), nor to non-C-related defect-induced features, since it does not appear in the spectrum of the As-doped sample (b), but seems to be directly related to the presence of carbon. Also, this feature disappears when carbon content becomes high enough to begin the formation of complexes. Thus, it seems reasonable to assume that this peak arises from a vibration of the C atom in a Ga cage, as a result of C entering the host lattice by substituting the N-atoms. A feature similar to this one is seen in the Raman spectrum of C-doped GaAs, and can be unambiguously attributed to a localized vibration of C atoms occupying As sites in the host GaAs lattice.[19–21] In this case the mode is a true localized vibration appearing at a frequency (582 cm^{-1}) well above the highest possible value for allowed vibrations of the host lattice (296 cm^{-1}). In our case, the identification is not quite as straightforward because the peak appears in the region of allowed GaN vibrations. However, knowing that the nearest-neighbor forces are the most important ones in determining the lattice vibrations, it is reasonable to expect that the peak should appear in about

the same frequency region in both materials, since in both cases it would result from C vibrations in a Ga cage. In order to justify this assignment a theoretical calculation using a valence force field (VFF) model was performed.

In order to determine the vibrational mode frequencies of carbon replacing N in cubic GaN we proceed as follows. First, the VFF method and the effective charge approximation for the long-range Coulomb interaction are used to carry out calculations of the phonon dispersion curves and phonon density of states of GaN. Bond-stretching and bond-bending force constants and nearest- and next-nearest-neighbors interactions are taken into account in the VFF phonon Hamiltonian.[22] Second, the Green's function technique is used to handle the perturbation introduced by the impurity. The relevant local density of states introduced by carbon is computed from the portion of the Green's function matrix, which covers the space of the defect, comprising the central carbon atom, its four nearest-neighbors (Ga) and 12 next-nearest-neighbors (N), in T_d symmetry.[23,24] The eigenvectors and eigenvalues of the Green's function matrix of the perturbed crystal are computed as a function of the force constants connecting carbon to its first neighbors. For suitable values of the force constants,[25] the calculation produces a resonance mode with T_2 symmetry, which would originate the line at 584 cm^{-1} in the Raman spectrum of our C-doped samples. The frequency of this mode is contained in the gap between the zone-center TO and LO modes and occurs at a point where the density of vibrational states is low. Thus, the results of the calculation strengthen the assignment of this Raman line as being the signature of the resonance vibration of a C atom occupying a N site in the GaN lattice.

HR-XRD ω-2θ scans of the (002) Bragg reflection of the GaN layers were taken in order to evaluate crystalline quality of the samples. Typical results from the undoped ($A1$ through $A3$), and two doped (D and G) samples are shown in Fig. 4 and its inset. The peak position (2θ) and the full width at half maximum (Γ) for each sample were obtained by fitting the experimental data by the least-squares method using pseudo-Voigt functions (shown by the solid lines in Fig. 4). The values of peak positions and linewidths obtained from this fit are listed in Table I. The peak positions are very similar in samples of comparable thicknesses and therefore, its value does not provide an indicator of differences in crystalline quality among them. On the other hand, linewidths vary considerably from one sample to the other and this can be used as a criterion to compare crystalline quality. Larger linewidths indicate a wider distribution of interplanar distances, resulting from poorer crystalline quality. In the inset of Fig. 4 we display data for undoped samples of different thicknesses. The linewidth of the thinnest sample (sample $A1$ with $d=185$ nm) is much larger than those of the thicker ones (samples $A2$ and $A3$ with $d>600$ nm), as can be seen by direct inspection of the figure or from the values of their linewidths listed in Table I. We believe that this is a consequence of stress relaxation and a reduction of stacking faults, which occurs as the GaN layer grows away from the substrate.[11] Sample $A2$ exhibits the smallest linewidth among the undoped samples and will be used as a reference sample when comparisons are made between doped and undoped samples. In the main part of the figure this reference sample is compared to two doped samples (D and G), chosen because they have, respectively, the smallest and largest linewidths of the samples under study (see Table I). Here we see that both C-doped samples have thinner lines and, therefore, better crystalline quality than the undoped reference sample. This evidence reinforces the picture of carbon incorporation suggested by the Raman data. Other optical measurements show significant evidence in the same direction. We shall discuss this evidence in what follows and postpone a quantitative discussion of linewidths vs carbon concentration until PLE data have been discussed.

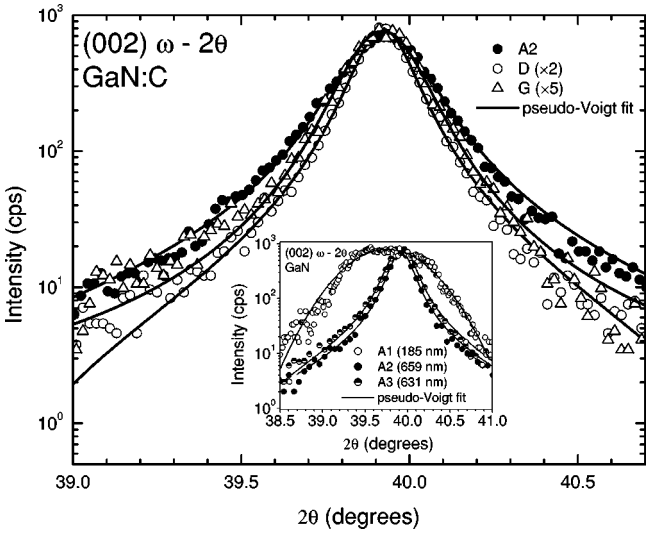

FIG. 4. High-resolution ω-2θ x-ray diffraction scans of the symmetric (002) reflex of cubic GaN for different C doping concentrations, as shown in Table I. Solid lines are fits to the experimental data using pseudo-Voigt functions. The main figure compares the reference undoped sample with two carbon-doped ones. The inset compares three undoped samples of different thicknesses.

The PL spectra of samples with different C content (including samples $A1$ and $A2$, with no intentional C doping) are shown in Fig. 5. No qualitative difference is found be-

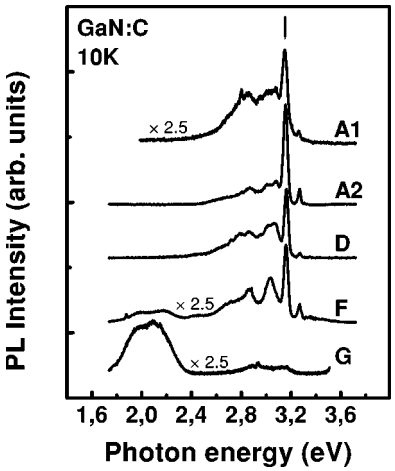

FIG. 5. PL spectra of representative undoped and C-doped cubic GaN with different carbon concentrations.

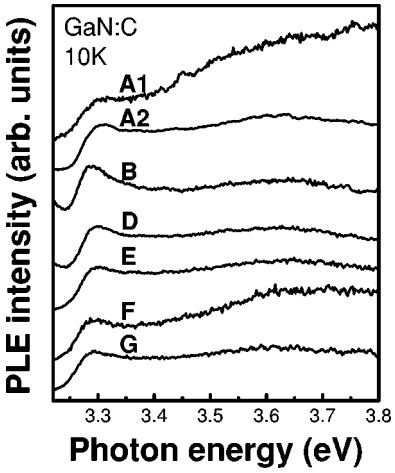

FIG. 6. PLE spectra of representative samples of cubic GaN films with and without carbon doping.

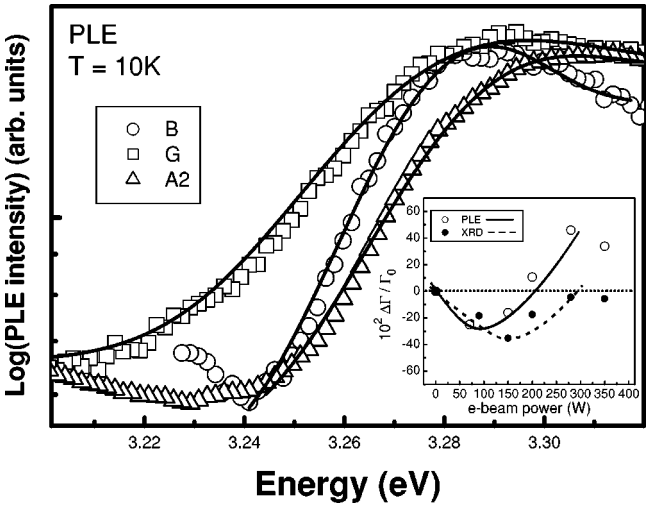

FIG. 7. Log plot of the absorption edges of three cubic GaN samples: The reference undoped sample $A2$ and the two C-doped samples with the smallest (B) and largest (G) linewidths (see Table I). The open symbols represent experimental data and the solid lines are least-square fits performed as explained in the text. The inset shows the behavior of the relative linewidth of PLE and XRD lines, represented by open and close circles, respectively. The solid and dotted lines are guides to the eye.

tween the spectra of the two undoped samples, just an improvement in the PL intensity when going from sample $A1$ to sample $A2$, in consonance with the results on crystalline quality shown by the XRD data. A detailed discussion on the relationship between carbon content and the PL spectra from carbon doped *c*-GaN samples can be found in Ref. 8. Here we shall concentrate our discussion around two features of these spectra. The first is the sharp peak at 3.15 eV, marked by the arrow in Fig. 5. This peak is attributed to donor-acceptor (D_0-A_0) transitions, occurring as well in all samples of cubic GaN not intentionally doped[26] or *n* doped.[8] In these samples there is always a residual acceptor concentration, attributed to the large dislocation density ($\sim 10^{11}$ cm^{-2}) present in the films, which are involved in the D_0-A_0 transition at 3.15 eV.[8,26] The second feature appears as carbon concentration increases and is composed of a broad structure around 2.1 eV. This structure grows in intensity as the C content increases and eventually dominates the spectrum for the most heavily doped samples. This feature is attributed by the author of Ref. 8 to the formation of a compensating dicarbon split-interstitial center, i.e., a complex formed by a carbon atom occupying a N site and a second C atom in an interstitial position. We want to highlight one particular aspect of the trends illustrated in Fig. 5; namely, the fact that in the C-doped samples, upon increasing the C concentration, the intensity of the original D_0-A_0 transition decreases and all but disappears for the most highly doped sample (Compare curves *D*, *F*, and *G* in Fig. 5). In principle, this can be caused by the disappearance of the donor levels resulting from heavy *p*-type doping. On the other hand, this is also consistent with the reduction of the lattice distortions provoked by the N vacancies. Since these distortions are thought to be responsible for the donor levels involved in the 3.15 eV transition, the reduction in their number would result in the observed decrease in intensity of this line. The latter interpretation is in agreement with the XRD and Raman results discussed in the previous paragraphs.

PLE spectra of representative samples, around the absorption edge region, are shown in Fig. 6. These spectra were obtained by centering the analyzing spectrometer at PL peaks well below the absorption edge of cubic GaN. For undoped and lightly doped samples, the best results were obtained when this centering was done at the PL peak of 2.86 eV. For the more heavily doped samples this centering was done around the C-complex band at 2.1 eV. The resulting PLE spectrum mimics the absorption spectra. For sample $A1$, it closely resembles a broadened step function, a line-shape characteristic of an M_0 singularity with an exciton that is broad enough to merge with the continuum.[27] Fitting this spectrum with a broadened step function, we obtain for the photon energy of the absorption edge and broadening parameter (full width at half maximum) the values: $E_g = 3.26$ eV and $\Gamma = 50$ meV, respectively.[27] The absorption edge profile of the other samples has the exciton well resolved from the continuum, as a result of their improved crystalline quality. This profile is well fitted with the combination of a Gaussian (exciton absorption) and broadened step function (continuum). The result of this procedure yields values for the excitonic and absorption edge critical energies (E_{exc} and E_g, respectively) and full widths at half maxima (Γ_{exc} and Γ_g). The parameters resulting from fitting the PLE spectra of all our samples are listed in Table I. The clear separation between exciton and continuum begins to blur as carbon concentration increases beyond a certain point, as a consequence of the increased broadening of the absorption edge. This is made explicit in Fig. 7, where the log of the absorption coefficient is plotted as a function of photon energy for the reference sample ($A2$, undoped) and for the doped samples having largest (sample G) and smallest (sample B) linewidths. In this figure, open symbols represent experimental data while continuous lines are least-squares fits to the data using the line shapes previously described. Visual inspection of this figure shows that for low carbon concentrations, the

absorption edge becomes sharper than in the undoped reference sample (compare curves for samples *B* and *A*2). For high carbon concentrations the opposite happens, as can be seen by comparing the curves of sample *G* with the other two. The evolution of the linewidth with carbon concentration can be followed systematically by examining the behavior of the function:

$$\frac{\Delta\Gamma}{\Gamma_0} = (\Gamma - \Gamma_0),$$

where Γ is the linewidth derived from the spectrum of a given sample and Γ_0 is the Γ obtained for the reference undoped sample *A*2. This definition allows the results from fitting the PLE and XRD spectra to be plotted in the same graph. In the inset of Fig. 7 we plot this relative variation in linewidth against *e*-beam power, which is a measure of carbon concentration (see Table I). Open (closed) dots are results obtained from the PLE (XRD) spectra of our samples. The solid (dotted) lines are meant to guide the eye and illustrate the overall trend. The data for both types of experiments follow the same general trend: $\Delta\Gamma/\Gamma_0$ initially decreases as carbon begins to be incorporated, passes through a minimum and then increases again as the carbon concentration continues to increase beyond this point. The PLE curve has a minimum at lower concentrations, and rises in a steeper manner after that, than the one corresponding to XRD data. The XRD curve correlates with the distribution of interplane distances and is, therefore, an indicator of the quality and regularity of the lattice. Hence, its minimum corresponds to the carbon concentration which produces the best crystalline quality. The broadening of the absorption coefficient, however, contains two distinct contributions: (i) a reduction in broadening resulting from improved crystalline quality and (ii) an increase in the broadening resulting from the formation of band tails associated with increasing concentrations of the doping impurity. The latter effect has been extensively discussed in the literature[28] and is more easily observed when plotting the log of the absorption coefficient versus photon energy (Fig. 7). The curve representing the relative difference in linewidth of the PLE data has its minimum before the carbon concentration reaches that corresponding to best crystallinity (minimum of the corresponding line for XRD data) because both contributions to the linewidth have opposite directions as carbon concentration increases. Beyond this point, the PLE curve rises more steeply than the XRD one because both contributions (band tails and decrease in crystalline quality) now combine to increase the linewidth. So the results from both types of measurements, PLE and XRD, are consistent with one another and with the picture suggested by the other optical measurements.

The results from all our measurements agree on the point that crystalline quality increases as carbon concentration increases, up to a certain critical value. Above this concentration crystalline quality begins to deteriorate again. This behavior is consistent with the picture of the way in which carbon impurities are incorporated in the GaN lattice during growth by rf-plasma assisted MBE, in which C atoms enter preferentially into the sites of N vacancies. This is not surprising in view of the similarity in size between C and N. Also, *ab initio* self-consistent electronic structure calculations show that the formation energy for carbon replacing N in GaN is much lower than when it replaces Ga or when it is incorporated interstitially.[29–31] However, as carbon concentration increases, C atoms begin to incorporate nonsubstitutionally and form complexes, degrading the crystalline quality once more.

IV. SUMMARY AND CONCLUSIONS

We have presented experimental HR-XRD and optical data that give a strong indication of the lattice sites occupied by carbon during growth of carbon doped cubic-GaN by rf-plasma assisted MBE on semi-insulating (001) GaAs. Although each result by itself gives merely a suggestive evidence, the agreement between the results of the four distinct types of measurements, supported by a model calculation in the case of the Raman results, form a compelling body of evidence in favor of the proposed picture. These results lead us to the following picture for the carbon incorporation into the *c*-GaN lattice: the C atoms initially enter the sites of N vacancies in the native material, thus improving its crystalline quality. The higher the *e*-beam power used during growth, and therefore the C concentration, the better the crystallinity of the sample, up to a critical power ($\sim$200 W in our system). At higher powers, C atoms begin to incorporate nonsubstitutionally and form complexes, degrading the crystalline quality once more.

ACKNOWLEDGMENTS

Financial support from the *Fundação de Amparo à Pesquisa do Estado de São Paulo* (FAPESP) (Grants No. 01/01067-4 and 98/12779-0) is gratefully acknowledged. The support from the *Conselho Nacional de Desenvolvimento Científico e tecnológico* (CNPq) and *Deutsche Forschungsgemeinschaft* (DFG) is also acknowledged. The authors would like to thank Professor J. C. Galzerani from *Universidade Federal de São Carlos* for the use of his laboratory and Dr. M. T. O. Silva for his help with the Raman experiments.

*Electronic address: jtsoares@if.usp.br

[1] S.F. Chichibu, A.C. Abare, M.P. Mack, M.S. Minsky, T. Deguchi, D. Cohen, P. Kozodoy, S.B. Fleischer, S. Keller, J.S. Speck, J.E. Bowers, and E. Hu, Mater. Sci. Eng., B **59**, 298 (1999).

[2] L.M.R. Scolfaro, Phys. Status Solidi A **15**, 190 (2002).

[3] H. Yang, L.X. Zheng, J.B. Li, X.J. Wang, D.P. Xu, Y.T. Wang, X.W. Hu, and P.D. Han, Appl. Phys. Lett. **74**, 2498 (1999).

[4] D.J. As, A. Richter, J. Busch, M. Lübbers, J. Minikes, and K. Lischka, Appl. Phys. Lett. **76**, 13 (2000).

[5] H. Gomez-Cuatzin, J. Tardy, P. Rojo-Romeo, A. Philippe, C. Bru

Chevalier, A. Souifi, G. Guillot, E. Martinez-Guerrero, G. Feuillet, B. Daudin, P. Aboughé-Nzé, and Y. Monteil, Phys. Status Solidi A **131**, 176 (1999).
[6] Y. Taniyasu, K. Suzuki, D.H. Lim, A.W. Jia, M. Shimotomai, Y. Kato, M. Kobayashi, A. Yoshikawa, and K. Takahashi, Phys. Status Solidi A **241**, 180 (2000).
[7] C.R. Abernathy, J.D. MacKenzie, S.J. Pearton, and W.S. Hobson, Appl. Phys. Lett. **66**, 1969 (1996).
[8] D.J. As, Defect Diffus. Forum **206–207**, 87 (2002).
[9] D.J. As and U. Köhler, J. Phys.: Condens. Matter **13**, 8923 (2001).
[10] D. Schikora, M. Hankeln, D.J. As, K. Lischka, T. Litz, A. Waag, T. Buhrow, and F. Henneberger, Phys. Rev. B **54**, R8381 (1996).
[11] D. J. As, in *III-Nitride Semiconductor Materials: Growth*, edited by M. O. Manasreh and I. T. Ferguson, Optoelectronic Properties of Semiconductors and Superlattices Vol. 19 (Gordon and Breach, New York, 2002), p. 323.
[12] A. Tabata, A.P. Lima, L.K. Teles, L.M.R. Scolfaro, J.R. Leite, V. Lemos, B. Schöttker, T. Frey, D. Schikora, and K. Lischka, Appl. Phys. Lett. **74**, 362 (1999).
[13] Y.A. Pusep, M.T.O. Silva, J.R.L. Fernandez, V.A. Chitta, J.R. Leite, T. Frey, D.J. As, D. Schikora, and K. Lischka, J. Appl. Phys. **91**, 6197 (2002).
[14] L.E. Ramos, J. Furthmüller, F. Bechstedt, L.M.R. Scolfaro, and J.R. Leite, J. Phys.: Condens. Matter **14**, 2577 (2002).
[15] P. Bogusławski, E.L. Briggs, and J. Bernholc, Phys. Rev. B **51**, 17255 (1995).
[16] For a more detailed discussion, see M.D. McCluskey, Appl. Phys. Lett. **87**, 3593 (2000); A.S. Barker, Jr. and A.J. Sievers, Rev. Mod. Phys. **47** (S2), FS1 (1975).
[17] H. Siegle, A. Kaschner, A. Hoffmann, I. Broser, C. Thomsen, S. Einfeldt, and D. Hommel, Phys. Rev. B **58**, 13 619 (1998).
[18] G. Kaczmarczyk, A. Kaschner, A. Hoffmann, and C. Thomsen, Phys. Rev. B **61**, 5353 (2000).
[19] R.C. Newman, F. Thompson, M. Hyliands, and R.F. Peast, Solid State Commun. **10**, 505 (1972).
[20] W.M. Theis, K.K. Bajaj, C.W. Litton, and W.G. Spitzer, Appl. Phys. Lett. **41**, 70 (1982).
[21] L.M.R. Scolfaro, R. Pintanel, V.M.S. Gomes, J.R. Leite, and A.S. Chaves, Phys. Rev. B **34**, 7135 (1986).
[22] A.M. Santos, E.C.F. da Silva, O.C. Noriega, H.W.L. Alves, J.L.A. Alves, and J.R. Leite, Phys. Status Solidi B **232**, 182 (2002).
[23] R.M. Feenstra, R.J. Hauenstein, and T.C. McGill, Phys. Rev. B **28**, 5793 (1983).
[24] J.R. Leite, E.C.F. da Silva, and A. Dal Pino, Jr., Mater. Sci. Forum **38–41**, 263 (1989).
[25] A detailed description of the steps undertaken to obtain such values will be given in a future publication by A. M. Santos *et al.*
[26] D.J. As, F. Schmilgus, C. Wang, B. Schotter, D. Schikora, and K. Lischka, Appl. Phys. Lett. **70**, 1311 (1997).
[27] J.R.L. Fernandez, O.C. Noriega, J.A.N.T. Soares, F. Cerdeira, E.A. Meneses, J.R. Leite, D.J. As, D. Schikora, and K. Lischka, Solid State Commun. **125**, 205 (2003).
[28] See, for example, J. I. Pankove, in *Optical Processes in Semiconductors* (Dover, New York, 1971), Chap. 3.
[29] J. Neugebauer and C.G. Van de Walle, Festkoerperprobleme **35**, 25 (1995).
[30] L.E. Ramos, J. Furthmueller, L.M.R. Scolfaro, J.R. Leite, and F. Bechstedt, Phys. Rev. B **66**, 075209 (2002).
[31] C.H. Seager, A.F. Wright, J. Yu, and W. Götz, J. Appl. Phys. **92**, 6553 (2002).